




# Improvement of Sn-3Ag-0.5Cu Soldered Joints Between $\text{Bi}_{0.5}\text{Sb}_{1.5}\text{Te}_3$ Thermoelectric Material and a Cu Electrode

TUNG-HAN CHUANG <sup>1,3</sup>, SHIH-WEN HSU,<sup>1</sup> YAN-CHENG LIN,<sup>2</sup>  
WEI-TING YEH,<sup>1</sup> CHUN-HAO CHEN,<sup>1</sup> PEI-ING LEE,<sup>1</sup> PO-CHING WU,<sup>1,2</sup>  
and HAO-PENG CHENG<sup>1</sup>

1.—Department of Materials Science and Engineering, National Taiwan University, Taipei 10617, Taiwan, ROC. 2.—Ag Materials Technology Co., LTD. (Amtc), Hsinchu 30078, Taiwan, ROC. 3.—e-mail: tunghan@ntu.edu.tw

A  $\text{Bi}_{0.5}\text{Sb}_{1.5}\text{Te}_3$  thermoelectric (TE) element was directly soldered to a Cu electrode using Sn-3Ag-0.5 Cu alloy. The interface was sound and the bonding strength was satisfactory (8.6 MPa). However, the solder layer was exhausted quickly during high-temperature storage (HTS) tests at 150°C for 300 h and 600 h, and the bonding strength drastically decreased to 1.5 MPa. The consumption of the solder was prevented by electroplating a Ni barrier layer on the TE element, though a low bonding strength of 1.9 MPa resulted. Adding a Sn-rich thin film and a Ni barrier layer onto the  $\text{Bi}_{0.5}\text{Sb}_{1.5}\text{Te}_3$  element led to a high bonding strength of 12.1 MPa, which decreased only slightly after HTS reliability tests at 150°C for 1000 h. The sound interfaces of the  $\text{Bi}_{0.5}\text{Sb}_{1.5}\text{Te}_3$ /Cu joints maintained their stability even after HTS at 175°C for 1000 h.

**Key words:**  $\text{Bi}_{0.5}\text{Sb}_{1.5}\text{Te}_3$  thermoelectric material, soldering, Ni barrier layer, high-temperature storage

## INTRODUCTION

Thermoelectric (TE) materials are used in applications such as power generators, heat dissipaters, active refrigerators, and industrial waste heat recyclers. However, the heat transfer of a single TE device is limited, so modules should be assembled by bonding multiple elements with metallic electrodes. The effectiveness of a TE module depends on the quality of the TE/electrode joint. Among the many techniques for bonding TE elements with metallic electrodes, brazing results in high bonding strength, and the brazed joints can endure high temperatures during the operation of the TE modules.<sup>1</sup> However, large thermal stress can accumulate at the joint interface or in the interior of the TE material during the brazing process and cause damage to the brazed TE module. An alternative is spark plasma sintering, but the high heating rate during the bonding

process can degrade the intrinsic properties of the TE materials.<sup>2</sup>

A newly developed method, the solid-liquid interdiffusion bonding (SLID) process, results in satisfactory bonding of Cu electrodes with various TE materials, such as BiTe,<sup>3</sup> PbTe,<sup>4</sup> and  $\text{Zn}_4\text{Sb}_3$ .<sup>5,6</sup> Although the SLID bonding process can also ensure high operating temperatures for TE modules, its intermetallic interlayer, having a thickness of only several  $\mu\text{m}$ , may cause co-planarity in the assembly of multiple TE elements. On the other hand, the traditional soldering process is widely used as an effective bonding method for electronic packaging.<sup>7</sup> It is also employed for the die bonding of light-emitting diode (LED) products<sup>8</sup> and recycling of sputtering targets.<sup>9</sup> For application in TE modules connected with metallic electrodes, soldering also exhibits certain advantages.<sup>10</sup> In comparison to the brazing and spark plasma sintering methods, soldering can be conducted at lower temperatures and thus induces less thermal stress. In addition, the liquid-phase solder at the TE/electrode interface has a much greater thickness than that of the interlayer

of the SLID bonding process, reducing the risk of coplanarity in assembly. For industrial applications, an optimized TE module can be achieved using a soldered joint at the cold end and a SLID joint at the hot end.

In many electronic products, Sn-3Ag-0.5Cu solder has been employed as a replacement for traditional Sn-37Pb solder alloy for environmental reasons. It also has superior strength, longer thermal fatigue life, improved creep resistance, and good wettability.<sup>11</sup> Chien et al.<sup>12</sup> produced a  $\text{Bi}_2\text{Te}_3/\text{Cu}$  soldered joint using Sn-3Ag-0.5Cu alloy for the study of electro-migration between the TE material and metallic electrode under current stressing. The Sn-3Ag-0.5Cu soldered joints in electronic packages also have satisfactory electrical conductivity despite certain intermetallic compounds that may appear at the interfaces.<sup>13</sup>

In this study, it was found that directly soldering the  $\text{Bi}_{0.5}\text{Sb}_{1.5}\text{Te}_3$  thermoelectric material with the Cu electrode using a Sn-3Ag-0.5Cu solder caused rapid consumption of the solder alloy, and various thick intermetallic compounds formed at the TE/solder interface after high-temperature storage (HTS) at 150°C for 300 h and 600 h, leading to poor bonding strength. The excessive intermetallic growth at the soldered interface was reduced by electroplating a Ni barrier layer on the  $\text{Bi}_{0.5}\text{Sb}_{1.5}\text{Te}_3$  surface. However, the  $\text{Bi}_{0.5}\text{Sb}_{1.5}\text{Te}_3/\text{Ni}/\text{Cu}$  soldered joint still had a low bonding strength due to the weak interaction between the  $\text{Bi}_{0.5}\text{Sb}_{1.5}\text{Te}_3$  thermoelectric material and the Ni barrier layer. Further improvement was achieved by pre-coating the element with a Sn thin film having a thickness of about 1  $\mu\text{m}$ , preheating the coated element at 250°C for 3 min, and electroplating a Ni barrier layer onto the Sn thin film. The pretreated  $\text{Bi}_{0.5}\text{Sb}_{1.5}\text{Te}_3$  thermoelectric element was then soldered with the Cu electrode using Sn-3Ag-0.5Cu solder. A satisfactory joint with high bonding strength was achieved in this case.

## EXPERIMENTAL

For this study, the  $\text{Bi}_{0.5}\text{Sb}_{1.5}\text{Te}_3$  thermoelectric material was prepared by vacuum melting at 750°C and zone refining with a speed of 1 mm/min. The  $\text{Bi}_{0.5}\text{Sb}_{1.5}\text{Te}_3$  ingot was then cut into TE elements with dimensions of 3 mm  $\times$  3 mm  $\times$  3 mm and ground with 4000-grit SiC paper. The TE element was bonded with a Cu electrode using a commercial Sn-3Ag-0.5Cu solder paste and reflowed according to the temperature profile shown in Fig. 1. Various modified soldering processes were employed to evaluate the improvements of the soldered interface and bonding strength. For this purpose, the interfaces of the  $\text{Bi}_{0.5}\text{Sb}_{1.5}\text{Te}_3/\text{Cu}$  soldered joints were observed via scanning electron microscopy (SEM), and the intermetallic compounds formed at the interfaces were analyzed by energy-dispersive x-ray spectroscopy (EDX) in the scanning electron

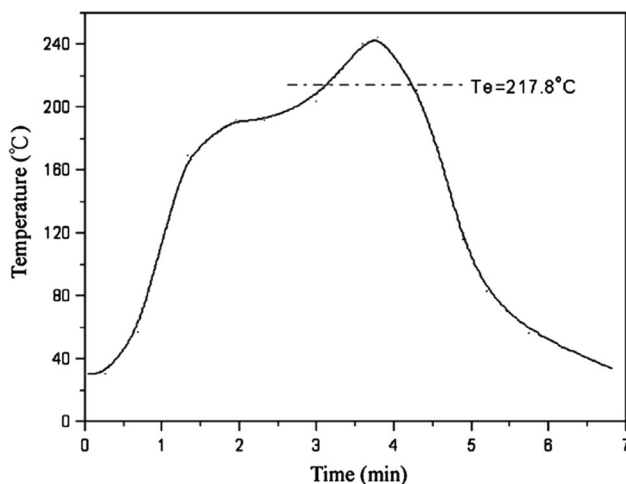


Fig. 1. Temperature profile for the soldering of  $\text{Bi}_{0.5}\text{Sb}_{1.5}\text{Te}_3/\text{Cu}$  joints using Sn-3Ag-0.5Cu alloy.

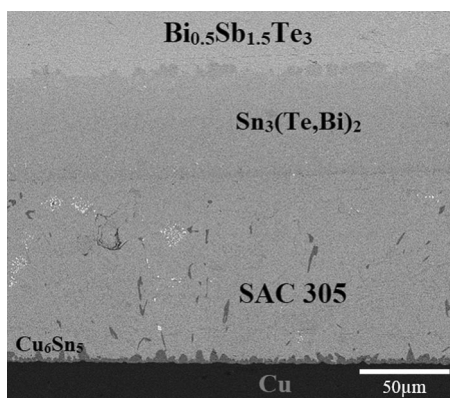


Fig. 2. Interfacial structure of a  $\text{Bi}_{0.5}\text{Sb}_{1.5}\text{Te}_3/\text{Cu}$  joint directly bonded with Sn-3Ag-0.5Cu solder.

microscope. The bonding strengths of various  $\text{Bi}_{0.5}\text{Sb}_{1.5}\text{Te}_3/\text{Cu}$  joints were shear tested with a DAGE 4000 bond tester at a speed of 0.3 mm/s. The fractured surfaces of the shear-tested specimens were also observed by SEM.

## RESULTS AND DISCUSSION

Figure 2 shows the interfacial morphology of a  $\text{Bi}_{0.5}\text{Sb}_{1.5}\text{Te}_3$  thermoelectric material directly bonded with a Cu electrode using a Sn-3Ag-0.5Cu solder. It can be seen that a thick layer of Sn (Te, Bi) phase with a composition (at.%) of Sn/Te/Bi = 60.5:36.9:2.6 formed at the SAC 305/ $\text{Bi}_{0.5}\text{Sb}_{1.5}\text{Te}_3$  interface. The formation of such a  $\text{Sn}_3(\text{Te}, \text{Bi})_2$  intermetallic compound at the SAC305/ $\text{Bi}_{0.5}\text{Sb}_{1.5}\text{Te}_3$  interface is consistent with the Bi-doped SnTe phase at the interfaces of Sn/Te and Sn-Bi/Te diffusion couples reported by Chen et al.<sup>14</sup> and Chiu et al.<sup>15</sup> Shear tests indicated a bonding strength of about 8.6 MPa in this case. After HTS testing of the SAC 305/ $\text{Bi}_{0.5}\text{Sb}_{1.5}\text{Te}_3$  soldered joint at 150°C for 300 h in an air furnace, the  $\text{Sn}_3(\text{Te}, \text{Bi})_2$  intermetallic layer had grown from 50  $\mu\text{m}$  to about 90  $\mu\text{m}$ , as shown in

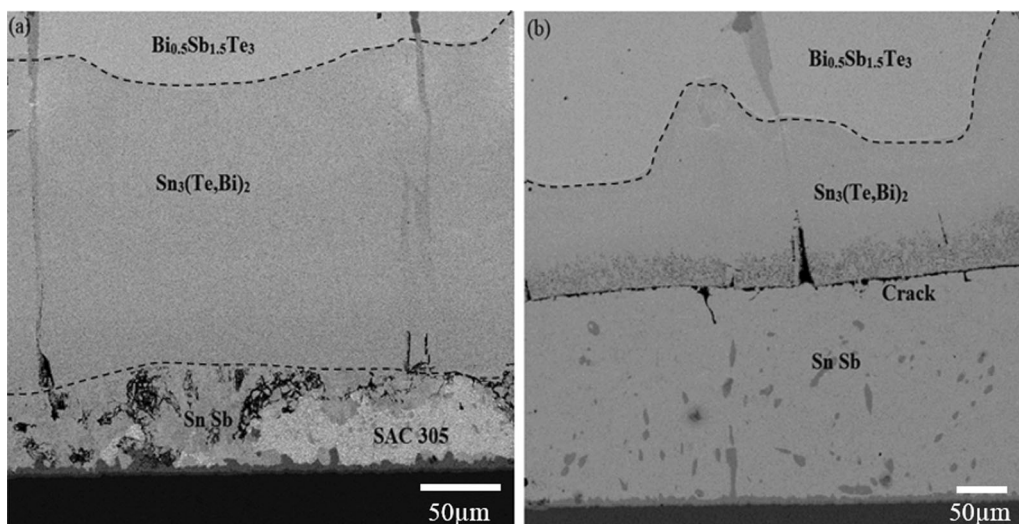


Fig. 3. Interfacial structures of  $\text{Bi}_{0.5}\text{Sb}_{1.5}\text{Te}_3/\text{Cu}$  joints soldered with Sn-3Ag-0.5Cu after high-temperature storage tests at  $150^\circ\text{C}$  for (a) 300 h and (b) 600 h.

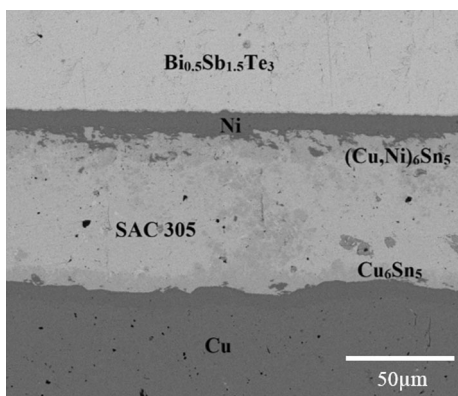


Fig. 4. Interfacial structure of a  $\text{Bi}_{0.5}\text{Sb}_{1.5}\text{Te}_3/\text{Cu}$  joint soldered with Sn-3Ag-0.5Cu using a Ni barrier layer.

Fig. 3a. Figure 3b shows that when the HTS time was increased to 600 h, the SAC 305 solder disappeared, and a 200- $\mu\text{m}$ -thick Sn-Sb intermetallic layer with a composition (at.%) of Sn/Sb = 54.1:45.9 formed between the  $\text{Sn}_3(\text{Te}, \text{Bi})_2$  and Cu electrode. In addition, a continuous crack was found at the  $\text{Sn}_3(\text{Te}, \text{Bi})_2/\text{Sn-Sb}$  interface. The shear strength of this  $\text{Bi}_{0.5}\text{Sb}_{1.5}\text{Te}_3/\text{Cu}$  joint dropped from 8.6 MPa to 1.5 MPa due to the SAC 305 solder being exhausted and the weak cohesion between the  $\text{Sn}_3(\text{Te}, \text{Bi})_2$  and Sn-Sb intermetallic layers.

To improve the soldered  $\text{Bi}_{0.5}\text{Sb}_{1.5}\text{Te}_3/\text{Cu}$  joints, an electroplated Ni layer with a thickness of about 7.5  $\mu\text{m}$  was employed as a diffusion barrier between the SAC 305 solder and the  $\text{Bi}_{0.5}\text{Sb}_{1.5}\text{Te}_3$  thermoelectric material. As shown in Fig. 4, a scallop-shaped layer with a composition (at.%) of Cu/Ni/

Sn = 49.5:5.0:45.5, corresponding to a  $(\text{Cu}, \text{Ni})_6\text{Sn}_5$  intermetallic phase, formed between the SAC 305 solder and the Ni barrier layer. In addition,  $\text{Cu}_6\text{Sn}_5/\text{Cu}_3\text{Sn}$  double layers appeared at the interface between the SAC 305 solder and Cu electrode, which is common in the reflow of Sn-based solder on Cu substrate in electronic packages.<sup>16</sup> The microstructures of the  $\text{Bi}_{0.5}\text{Sb}_{1.5}\text{Te}_3/\text{Cu}$  joints after HTS tests at  $120\text{--}175^\circ\text{C}$  for 500 h are shown in Fig. 5a, b, and c. As can be seen in those figures, the thickness of the Ni barrier layers decreased, while the interfaces remained similar to those of the as-soldered specimens shown in Fig. 4. However, it can be observed in Fig. 5d that large voids and cracks formed in the matrix of the SAC 305 solder after an HTS test at  $200^\circ\text{C}$  for 500 h. After an HTS test for 1000 h at  $120^\circ\text{C}$ , a large crack appeared at the  $\text{Bi}_{0.5}\text{Sb}_{1.5}\text{Te}_3/\text{Ni}$  interface, and the crack became continuous along the  $\text{Bi}_{0.5}\text{Sb}_{1.5}\text{Te}_3/\text{Ni}$  interface after an HTS test at  $150^\circ\text{C}$  for 1000 h, as shown in Fig. 6a and b, respectively. As shown in Fig. 6c, continuous cracks formed at the upper  $(\text{Cu}, \text{Ni})_6\text{Sn}_5/\text{SAC 305}$  and lower SAC 305/ $\text{Cu}_6\text{Sn}_5$  interfaces. Although the addition of a Ni barrier layer to the soldered  $\text{Bi}_{0.5}\text{Sb}_{1.5}\text{Te}_3/\text{Cu}$  joints resulted in sound interfaces after HTS tests of  $120^\circ\text{C}$  and  $175^\circ\text{C}$  for 500 h, the bonding strengths were only about 1.9 MPa, which could be attributed to the weak cohesion between the  $\text{Bi}_{0.5}\text{Sb}_{1.5}\text{Te}_3$  thermoelectric material and the Ni barrier layer. In fact, after shear tests, the fracture surfaces of the soldered  $\text{Bi}_{0.5}\text{Sb}_{1.5}\text{Te}_3/\text{Cu}$  joints formed with the Ni barrier layer revealed separation of the  $\text{Bi}_{0.5}\text{Sb}_{1.5}\text{Te}_3$  and Ni surfaces, as shown in Fig. 7a and b, respectively, which confirmed the inference of the fracture mode in this case. In fact, it

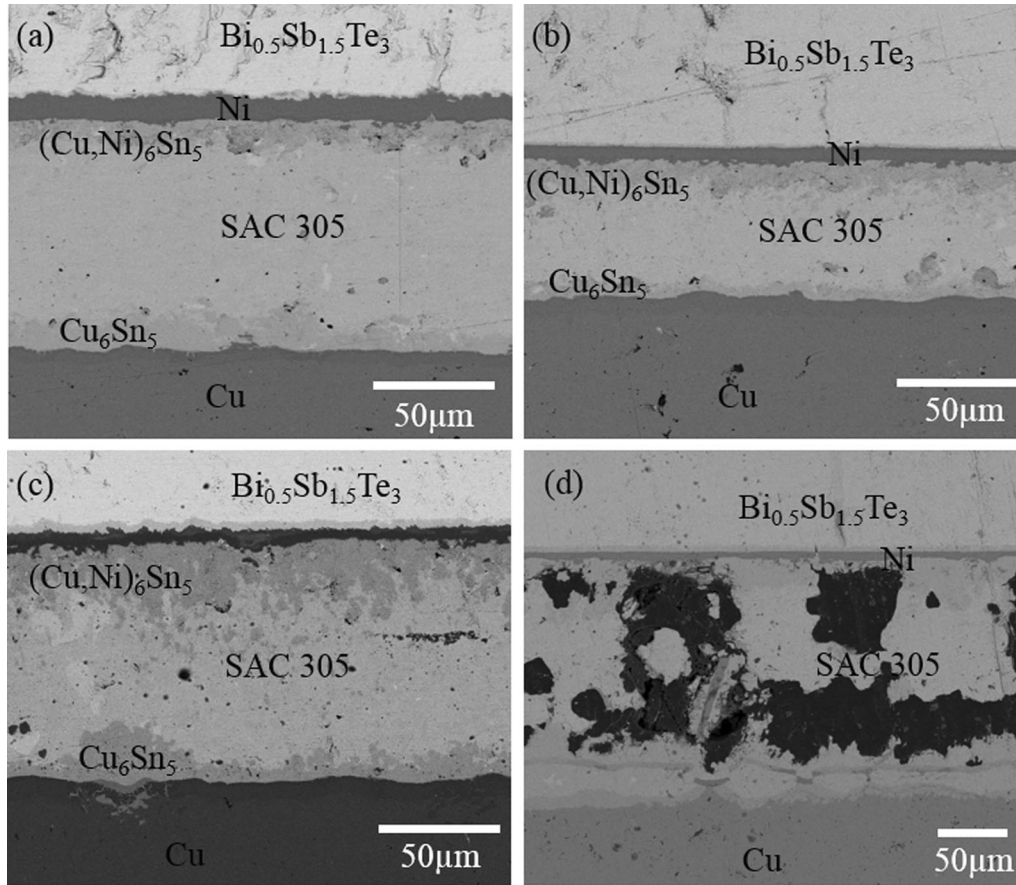


Fig. 5. Interfacial structures of  $\text{Bi}_{0.5}\text{Sb}_{1.5}\text{Te}_3/\text{Cu}$  joints soldered with Sn-3Ag-0.5Cu using a Ni-P barrier layer after high-temperature storage tests at various temperatures for 500 h: (a) 120°C, (b) 150°C, (c) 175°C, (d) 200°C.

can be seen in Fig. 8 that a reaction layer with a composition (at.%) of Ni/Te/Se = 62.1:32.1:5.8, corresponding to a  $\text{Ni}_3(\text{Te, Se})_2$  intermetallic phase, appeared at the soldered interface between the  $\text{Bi}_{0.5}\text{Sb}_{1.5}\text{Te}_3$  thermoelectric material and the Ni barrier layer after HTS tests at temperatures higher than 150°C for 500 h and 1000 h. The interfacial reaction did not yield a beneficial effect for the  $\text{Bi}_{0.5}\text{Sb}_{1.5}\text{Te}_3/\text{Cu}$  joints soldered with SAC 305. The failure of the Ni barrier was also reported by Lin et al., who found that a NiTe intermetallic compound layer formed between the Ni layer and  $\text{Bi}_2\text{Te}_3$  in a Ag (10  $\mu\text{m}$ )/Au (2  $\mu\text{m}$ )/Ni(5  $\mu\text{m}$ )/ $\text{Bi}_2\text{Te}_3$  joint after aging at 250°C for 10 h.<sup>17</sup> The mechanical weakness of the NiTe intermetallic compound led to the fracture of this multilayer structure.

For the solid-liquid interdiffusion bonding of a  $\text{Bi}_{0.5}\text{Sb}_{1.5}\text{Te}_3$  thermoelectric element with a Cu electrode using a Sn-rich thin film interlayer in a previous study,<sup>18</sup> the cohesion between the TE material and Ni barrier was enhanced by pre-coating a Sn-reactive layer on the surface of the  $\text{Bi}_{0.5}\text{Sb}_{1.5}\text{Te}_3$  thermoelectric element. The beneficial

effect of pre-coating a Sn thin film on the  $\text{Bi}_{0.5}\text{Sb}_{1.5}\text{Te}_3$  material to improve the TE/Ni interface was also confirmed for a SLID-bonded  $\text{Bi}_{0.5}\text{Sb}_{1.5}\text{Te}_3/\text{Cu}$  couple using an In interlayer.<sup>19</sup> A similar process was conducted for soldering  $\text{Bi}_{0.5}\text{Sb}_{1.5}\text{Te}_3/\text{Cu}$  joints with a Ni barrier layer: The  $\text{Bi}_{0.5}\text{Sb}_{1.5}\text{Te}_3$  specimens were electroplated with a 1- $\mu\text{m}$ -thick Sn layer and heated at 250°C under  $10^{-4}$  Pa vacuum for 3 min. While being heated, the electroplated Sn layer reacted with the  $\text{Bi}_{0.5}\text{Sb}_{1.5}\text{Te}_3$  material and was transformed into a continuous Sn-Sb-Bi layer embedded with many Sn-Te-Bi islands having compositions similar to those reported in previous studies on the SLID bonding of  $\text{Bi}_{0.5}\text{Sb}_{1.5}\text{Te}_3/\text{Cu}$  couples.<sup>18,19</sup> The bonding surface of this pretreated  $\text{Bi}_{0.5}\text{Sb}_{1.5}\text{Te}_3$  element was then electroplated with a 10- $\mu\text{m}$ -thick Ni barrier layer and soldered with SAC 305 alloy. The resultant interfacial structure of the  $\text{Bi}_{0.5}\text{Sb}_{1.5}\text{Te}_3/\text{Cu}$  joint is shown in Fig. 9a. As shown in the higher magnification of the soldered  $\text{Bi}_{0.5}\text{Sb}_{1.5}\text{Te}_3/\text{Ni}$  interface in Fig. 9b, a Te-Bi-Sb/Sn-Te-Bi/Sb-Bi-Ni sandwich structure formed between the  $\text{Bi}_{0.5}\text{Sb}_{1.5}\text{Te}_3$  thermo-

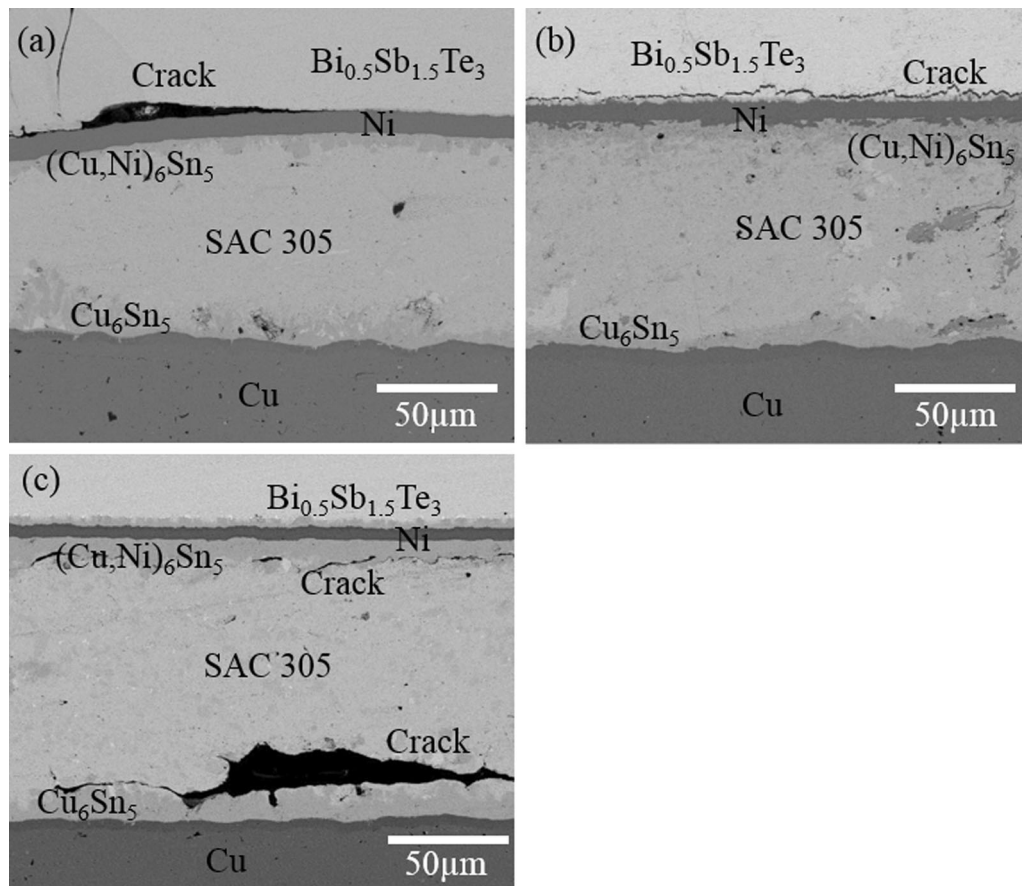


Fig. 6. Interfacial structures of  $\text{Bi}_{0.5}\text{Sb}_{1.5}\text{Te}_3/\text{Cu}$  joints soldered with Sn-3Ag-0.5Cu using a Ni-P barrier layer after high-temperature storage tests at various temperatures for 1000 h: (a) 120°C, (b) 150°C, (c) 175°C.

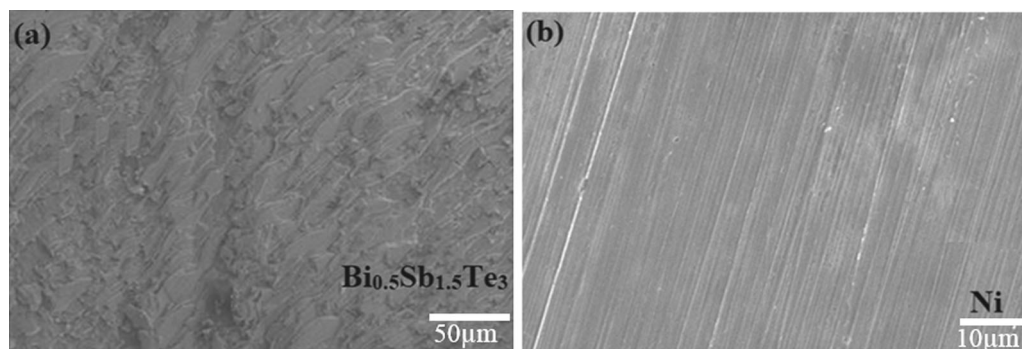


Fig. 7. Fracture surfaces of  $\text{Bi}_{0.5}\text{Sb}_{1.5}\text{Te}_3/\text{Cu}$  joints soldered with Sn-3Ag-0.5Cu using a Ni barrier layer after shear tests: (a) thermoelectric element side, (b) Cu electrode side.

electric material and the Ni barrier layer. The upper Te-Bi-Sb and Sb-Bi-Ni thin layers had a composition (at.%) of Te/Bi/Sb = 51.0:29.9:19.1, corresponding to a (Bi, Sb)Te intermetallic phase, and the lower Sb-Bi-Ni thin layer had a composition (at.%) of Sb/Bi/Ni = 60.0:20.2:19.8, corresponding to a  $(\text{Ni, Bi})_2\text{Sb}_3$  intermetallic phase. In addition, the thick Sn-Te-Bi

layer between the (Bi, Sb)Te and  $(\text{Ni, Bi})_2\text{Sb}_3$  thin films revealed a composition (at.%) of Te/Sn/Bi = 48.9:45.7:5.4, corresponding to a Te (Sn, Bi) intermetallic phase. The bonding strength of this  $\text{Bi}_{0.5}\text{Sb}_{1.5}\text{Te}_3/\text{Cu}$  joint, soldered with this modified method of pre-coating a Sn-rich interlayer between the  $\text{Bi}_{0.5}\text{Sb}_{1.5}\text{Te}_3$  TE element and the Ni barrier,

increased to a satisfactory value of 12.1 MPa, which is higher than those of  $\text{Bi}_{0.5}\text{Sb}_{1.5}\text{Te}_3/\text{Cu}$  joints SLID-bonded under optimized conditions using a Sn interlayer (10.7 MPa)<sup>18</sup> and an In interlayer (11.7 MPa)<sup>19</sup> in previous studies. The fractography shown in Fig. 10 evidenced that the fracture path changed to the interior of the  $\text{Bi}_{0.5}\text{Sb}_{1.5}\text{Te}_3$  materials, indicating that the cohesion at the TE/Ni interface had been effectively improved.

High-temperature storage tests of this SAC 305 soldered  $\text{Bi}_{0.5}\text{Sb}_{1.5}\text{Te}_3/\text{Cu}$  joint pre-coated with a Sn-rich layer and a Ni barrier layer were also conducted at 150°C in air for 300–1000 h. Figure 11 reveals that the interfacial structures of the specimens aged for various times remained almost unchanged. In addition, the bonding strengths decreased only slightly from 12.1 MPa for the as-soldered specimen to 11.0 MPa after the HTS tests at 150°C for 1000 h, as shown in Fig. 12. To confirm the sound reliability of  $\text{Bi}_{0.5}\text{Sb}_{1.5}\text{Te}_3/\text{Cu}$  joints soldered with this modified process, the specimens were aged at temperatures of 120–200°C for 500 h. Figure 13 shows that the interfaces of these soldered TE specimens did not fail after HTS tests

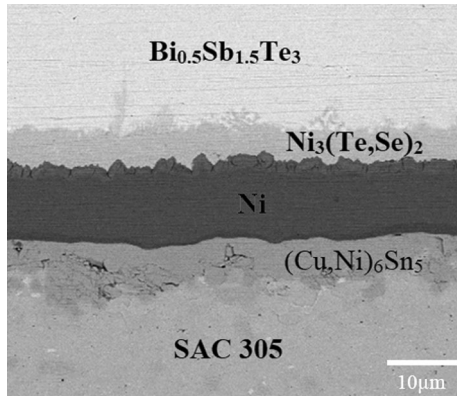


Fig. 8.  $\text{Ni}_3(\text{Te}, \text{Se})_2$  intermetallic layer between the  $\text{Bi}_{0.5}\text{Sb}_{1.5}\text{Te}_3$  thermoelectric element and the Ni barrier after soldering and high-temperature storage tests at 150°C for 500 h.

conducted at lower than 175°C, but damage resulted during tests at 200°C. The  $\text{Bi}_2\text{Te}_{2.55}\text{Se}_{0.45}/\text{Cu}$  joints survived even after long-term HTS tests at temperatures below 175°C for 1000 h, as evidenced in Fig. 14b.

## CONCLUSIONS

A  $\text{Bi}_{0.5}\text{Sb}_{1.5}\text{Te}_3$  thermoelectric material was bonded with a Cu electrode using a Sn-3Ag-0.5Cu solder. Although directly soldering the TE element to the Cu electrode resulted in a sound interface and satisfactory bonding strength of 8.6 MPa, the solder was exhausted quickly during high-temperature storage tests at 150°C for 300 h and 600 h, and the bonding strength drastically decreased to 1.5 MPa. The addition of a 10- $\mu\text{m}$ -thick Ni barrier between the  $\text{Bi}_{0.5}\text{Sb}_{1.5}\text{Te}_3$  thermoelectric element and the SAC 305 solder prevented the consumption of the solder alloy, and sound interfaces remained after soldering and after HTS reliability tests at temperatures of up to 175°C for 500 h. However, due to the weak cohesion between the thermoelectric material and the Ni barrier, the bonding strength was only 1.9 MPa. The  $\text{Bi}_{0.5}\text{Sb}_{1.5}\text{Te}_3/\text{Cu}$



Fig. 10. Fracture surface of a  $\text{Bi}_{0.5}\text{Sb}_{1.5}\text{Te}_3/\text{Cu}$  joint soldered with Sn-3Ag-0.5Cu with an inserted sandwich structure of Sn-rich alloy thin films and a Ni barrier layer.

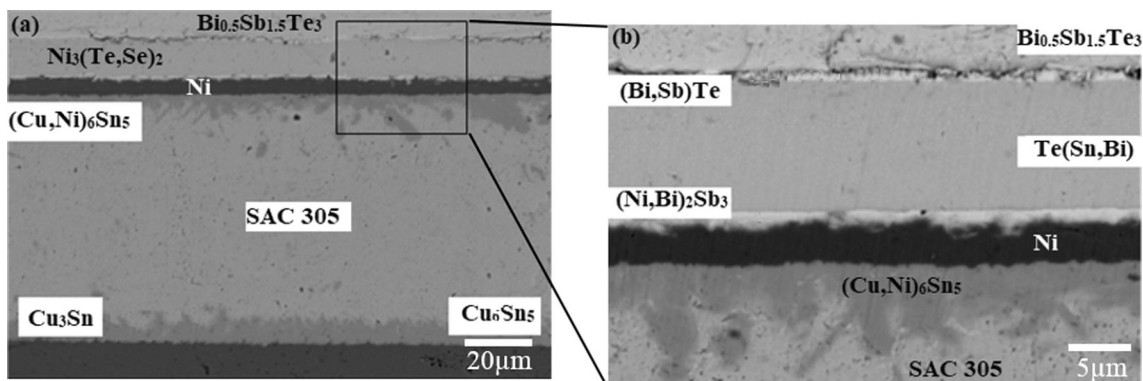


Fig. 9. (a) Interfacial structure of a  $\text{Bi}_{0.5}\text{Sb}_{1.5}\text{Te}_3/\text{Cu}$  joint soldered with Sn-3Ag-0.5Cu with an inserted sandwich structure of Sn-rich alloy thin films and a Ni barrier layer, (b) higher magnification of the soldered  $\text{Bi}_{0.5}\text{Sb}_{1.5}\text{Te}_3/\text{Ni}$  interface.

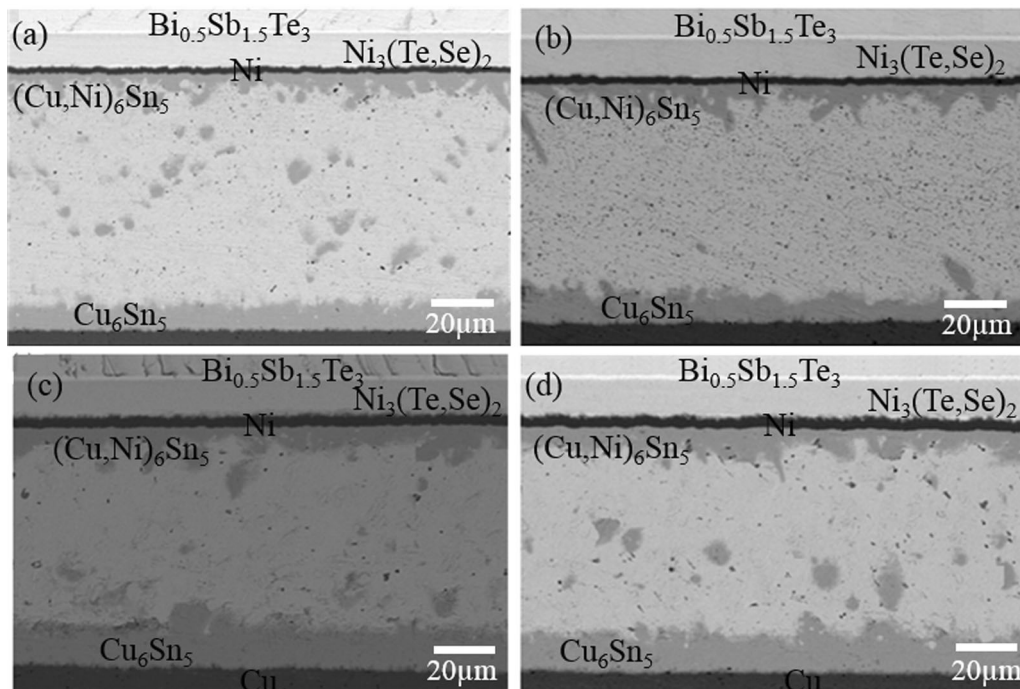


Fig. 11. Interfacial structures of  $\text{Bi}_{0.5}\text{Sb}_{1.5}\text{Te}_3/\text{Cu}$  joints soldered with Sn-3Ag-0.5Cu with an inserted sandwich structure of Sn-rich alloy thin films and a Ni barrier layer after HTS tests at  $150^\circ\text{C}$  for various times: (a) 300 h, (b) 600 h, (c) 800 h, (d) 1000 h.

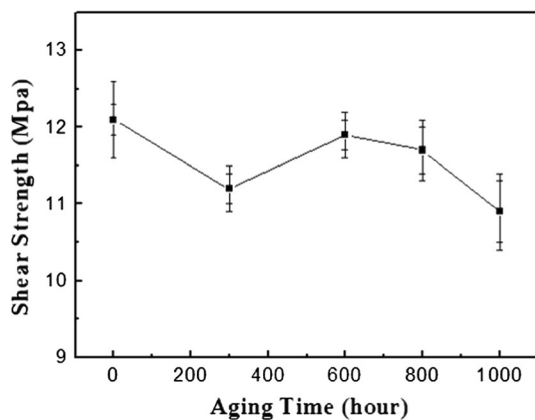


Fig. 12. Bonding strengths of  $\text{Bi}_{0.5}\text{Sb}_{1.5}\text{Te}_3/\text{Cu}$  joints soldered with Sn-3Ag-0.5Cu with an inserted sandwich structure of Sn-rich alloy thin films and a Ni barrier layer after HTS tests at  $150^\circ\text{C}$  for various times.

joints fractured along the interface between the  $\text{Bi}_{0.5}\text{Sb}_{1.5}\text{Te}_3$  element and the Ni barrier after shear tests. Increasing the HTS test time to 1000 h caused continuous cracks to appear at the bonding interfaces, further decreasing the bonding strength. Pre-coating the  $\text{Bi}_{0.5}\text{Sb}_{1.5}\text{Te}_3$  element with a  $1\text{-}\mu\text{m}$ -thick Sn layer and heating it at  $250^\circ\text{C}$  under  $10^{-4}$  Pa vacuum for 3 min led to the formation of a Sn-rich thin film on the TE surface. Further electroplating a Ni barrier on the pretreated  $\text{Bi}_{0.5}\text{Sb}_{1.5}\text{Te}_3$  thermoelectric element and soldering it with SAC 305 alloy resulted in a satisfactory bonding strength of 12.1 MPa. The fracture path of the  $\text{Bi}_{0.5}\text{Sb}_{1.5}\text{Te}_3/\text{Cu}$  joints after shear tests changed to the  $\text{Bi}_{0.5}\text{Sb}_{1.5}\text{Te}_3$  matrix. The interfacial structure of the soldered  $\text{Bi}_{0.5}\text{Sb}_{1.5}\text{Te}_3/\text{Cu}$  joints remained almost unchanged, and their bonding strengths decreased only slightly after HTS tests at temperatures up to  $175^\circ\text{C}$  for 1000 h.

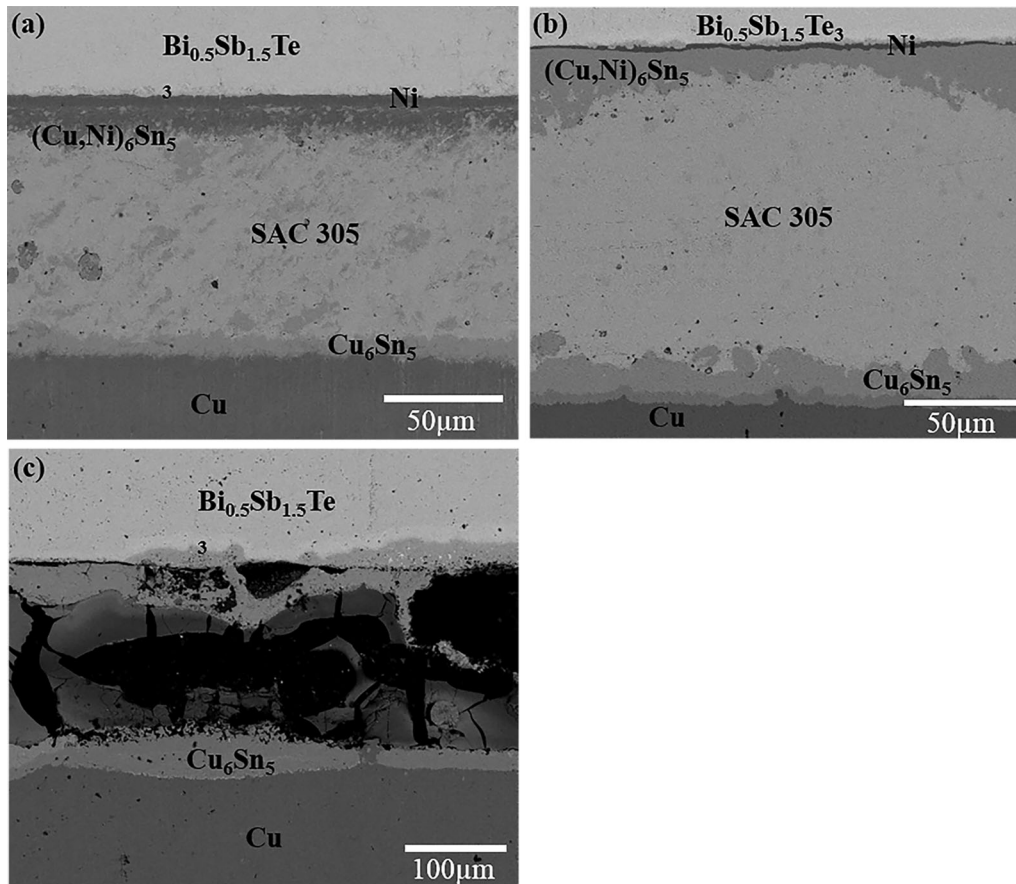


Fig. 13. Interfacial structures of  $\text{Bi}_{0.5}\text{Sb}_{1.5}\text{Te}_3/\text{Cu}$  joints soldered with Sn-3Ag-0.5Cu with an inserted sandwich structure of Sn-rich alloy thin films and a Ni barrier layer after HTS tests at various temperatures for 500 h: (a) 120°C, (b) 175°C, (c) 200°C.

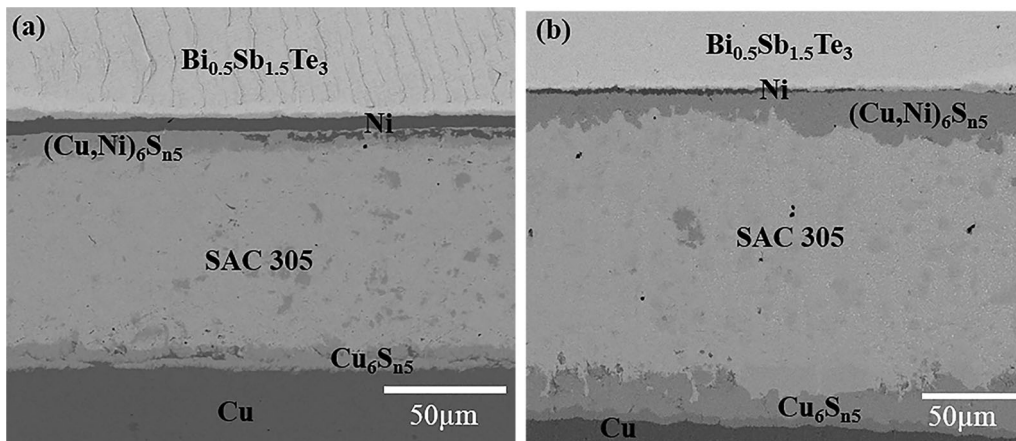


Fig. 14. Interfacial structures of  $\text{Bi}_{0.5}\text{Sb}_{1.5}\text{Te}_3/\text{Cu}$  joints soldered with Sn-3Ag-0.5Cu with an inserted sandwich structure of Sn-rich alloy thin films and a Ni barrier layer after HTS tests at various temperatures for 1000 h: (a) 120°C, (b) 175°C.

## ACKNOWLEDGMENTS

This study was sponsored by the Ministry of Science and Technology, Taiwan, under grant no. MOST 108-2221-E-002-094.

## REFERENCES

1. R. Zybala, K.T. Wojciechowski, M. Schmidt, and R. Mania, *Mater. Ceram.* 62, 481 (2010).
2. W. Xie, X. Tang, Y. Yan, Q. Zhang, and T.M. Tritt, *Appl. Phys. Lett.* 94, 102 (2009).
3. C.H. Chuang, Y.C. Lin, and C.W. Lin, *Metals* 6, 92 (2016).
4. T.H. Chuang, H.J. Lin, C.H. Chuang, W.T. Yeh, J.D. Hwang, and H.S. Chu, *J. Electron. Mater.* 43, 4610 (2014).
5. Y.C. Lin, K.T. Lee, J.D. Hwang, H.S. Chu, C.C. Hsu, S.C. Chen, and T.H. Chuang, *J. Electron. Mater.* 45, 4935 (2016).
6. L.W. Chen, C. Wang, Y.C. Liao, C.L. Li, T.H. Chuang, and C.H. Hsueh, *J. Alloys Compd.* 762, 631 (2018).



7. R.R. Tummala and E.J. Rymaszewski, *Microelectronics Packaging Handbook* (New York: Van Nostrand Reinhold, 1989), pp. 80–81.
8. G. Elger, M. Hutter, H. Oppermann, R. Aschenbrenner, H. Reichl, and E. Jager, *Microsyst. Technol.* **7**, 239 (2002).
9. F. Hillen, D. Pickart-Castillo, and J. Rass, *Weld. Cut.* **52**, E162 (2000).
10. H. Zhang, H.Y. Jing, Y.D. Han, L.Y. Xu, and G.-Q. Lu, *J. Alloys Compd.* **576**, 424 (2013).
11. K. Zeng and K.N. Tu, *Mater. Sci. Eng. R* **38**, 55 (2002).
12. P.Y. Chien, C.H. Yeh, H.H. Hsu, and A.T. Wu, *J. Electron. Mater.* **43**, 284 (2014).
13. R.J. Fields, S.R. Low III, and G.K. Lecey, Jr., Metal science of joining, in *Proceedings of TMS Symposium, Cincinnati, USA*, Oct 20–24, 1991.
14. S.W. Chen and C.N. Chiu, *Scripta Mater.* **56**, 97 (2007).
15. C.N. Chiu, C.H. Wang, and S.W. Chen, *J. Electron. Mater.* **37**, 40 (2007).
16. T.H. Chuang, H.M. Wu, M.D. Cheng, S.Y. Chang, and S.F. Yen, *J. Electron. Mater.* **33**, 22 (2004).
17. W.P. Lin, D.E. Wesolowski, and C.C. Lee, *J. Mater. Sci. Mater. Electron.* **22**, 1313 (2011).
18. C.L. Yang, H.J. Lai, J.D. Hwang, and T.H. Chuang, *J. Mater. Eng. Perform.* **22**, 2029 (2013).
19. Y.C. Lin, C.L. Yang, J.Y. Huang, C.C. Jain, J.D. Hwang, H.S. Chu, S.C. Chen, and T.H. Chuang, *Metall. Mater. Trans.* **47A**, 4767 (2016).

**Publisher's Note** Springer Nature remains neutral with regard to jurisdictional claims in published maps and institutional affiliations.